CFD Letters

Penerbit Akademia Baru

CFD Letters

Effects of Mixed Convection on Methanol and Kerosene Oil Based Micropolar Nanofluid Containing Oxide Nanoparticles

Open Access

Hamzeh T. Alkasasbeh[1], Mohammed Z. Swalmeh[2,3], Abid Hussanan[4,5,*], Mustafa Mamat[2]

[1] Department of Mathematics, Faculty of Science, Ajloun National University, P.O. Box 43, Ajloun 26810, Jordan
[2] Faculty of Informatics and Computing, Universiti Sultan Zainal Abidin (Kampus Gong Badak), 21300 Kuala Terengganu, Terengganu, Malaysia
[3] Faculty of Arts and Sciences, Aqaba University of Technology, Aqaba, Jordan
[4] Division of Computational Mathematics and Engineering, Institute for Computational Science, Ton Duc Thang University, Ho Chi Minh City 700000, Vietnam
[5] Faculty of Mathematics and Statistics, Ton Duc Thang University, Ho Chi Minh City 700000, Vietnam

ARTICLE INFO

ABSTRACT

The purpose of this communication is to examine the micro-rotation and micro-inertia characteristics of nanofluids over a solid sphere under mixed convection effect. Two types of oxide nanoparticles namely graphene and iron oxide suspended in two different types of base fluids such as methanol and kerosene oil. The governing boundary layer equations are transformed into nonlinear partial differential equations system and solved numerically using an implicit finite difference scheme known as Keller box method. The results for temperature, velocity and angular velocity are discussed and plotted for different values of the parameters, namely, nanoparticle volume fraction, the micro-rotation parameter and the mixed convection parameter by considering the thermo-physical properties of both nanoparticles and base fluids. Moreover, numerical results for the local Nusselt number and the local skin friction coefficient are obtained. It is found that Fe_3O_4/GO kerosene oil has higher in local Nusselt number compared with Fe_3O_4/GO methanol. The results of the local Nusselt number and the local skin friction for the Newtonian fluid are found to be in good accurate with the literature.

1. Introduction

A nanofluid is a heat-transfer fluid [1] containing nanoparticles with a size smaller than 100 nm such as oxides, metals and carbides [2]. Common base fluids comprise water oil and ethylene glycol [3], The nanoparticles has a unique chemical and physical properties, while compared only to base fluid, will increase the efficiency of the thermal conductivity and the convective heat-transfer coefficient [4]. Nanofluids have many properties that make them potentially useful in several applications in heat transfer, such as microelectronics, fuel cells, pharmaceutical processes, and hybrid-powered engines. Buongiorno [5] published an article on the convective transport in

---

* Corresponding author.
  abidhussanan@tdtu.edu.vn (Abid Hussanan)

nanofluids. The nanofluid flow inside two-sided lid-driven differentially heated square cavity is studied numerically by Tiwari *et al.,* [6]. The nanofluids used to acquire optimum thermal properties at the lowest volume fraction of nanoparticles in the base fluid by Godson *et al.,* [7]. Kandelousi *et al.,* [8] also considered the nanofluid flow and heat transfer through a permeable channel. Haq *et al.,* [9] studied the slip effect on heat transfer nanofluid flow past a stretching surface. There are several references that have on nanofluid as in the universal book by Das *et al.,* [1], and many studies that have been conducted to boost the heat-transfer characteristics technique by nanofluids, including some several study [10-16].

The classical Navier-Stokes theory described the flow properties of non-Newtonian materials, but this theory wasn't suitable to describe microrotations, certain microscopic effects growing from the local structure of fluid elements, and some naturally arising fluids, which are known as micropolar or thermomicropolar fluids. Micropolar fluid theory and its dilation to thermomicropolar fluids was initially introduced by Eringen *et al.,* [17]. Further, many physicists, engineers and mathematicians have been studied on the micropolar fluid to conclude the different results related to flow problems. Hassanien *et al.,* [18] presented the boundary layer flow and heat transfer from a stretching sheet to a micropolar fluid. Papautsky *et al.,* [19] investigated the laminar fluid behaviour in microchannels using micropolar fluid theory. Nazar *et al.,* [20] considered stagnation point flow of a micropolar fluid towards a stretching sheet. Exact solutions are obtained using the Laplace transform technique for the unsteady flow of a micropolar fluid by Sherief *et al.,* [21]. Hussanan *et al.,* [22] described the microrotation, temperature, velocity and concentration are considered. Hussanan *et al.,* [23] explained the unsteady natural convection flow of a micropolar fluid on a vertical plate oscillating in its plane with Newtonian heating condition. Free convection boundary layer flow of micropolar fluid on a solid sphere with convective boundary conditions was considered by Alkasasbeh *et al.,* [24]. Alkasasbeh [25] explores heat transfer magnetohydrodynamic flow of micropolar Casson fluid on a horizontal circular cylinder with thermal radiation. Natural convection on boundary layer flow of Cu-water and Al_2O_3-water micropolar nanofluid about a solid sphere investigated by Swalmeh *et al.,* [26] and micropolar forced convection flow over moving surface under magnetic field was inspected by Waqas *et al.,* [27].

The heat transfer through a boundary layer in the mixed convection flow about a sphere has a vast space in applied technology, such as solving the cooling problems in turbine blades, electronic systems and manufacturing processes. Experiments on heat transfer between spheres and airflow Yuge, [28]. Recently, the various papers in mixed convection boundary-layer flow for an isothermal solid sphere with different types of fluids, was presented by some researcher [29-33].

The aim of this present paper is to study the mixed convection boundary layer flow over a solid sphere in a micropolar nanofluid with constant wall temperature. Iron oxide (Fe_2O_4) and graphene (GO) in two based micropolar nanofluid (methanol and kerosene oil) have been considered in the present investigation. The boundary-layer equations are solved numerically via efficient implicit finite-difference scheme known as the Keller-box method, as displayed by Cebeci *et al.,* [34]. The effects of the nanoparticle volume fraction parameters, the mixed convection and micro-rotation parameter on the local heat transfer, local skin friction, temperature, velocity and angular velocity around the sphere are discussed and explained in the tables and figures. For comparison purposes, the present results for $\chi = 0$ and $K = 0$ (regular Newtonian fluid) and Pr = 0.7 are computed, and they show excellent agreement with those obtained by Nazar *et al.,* [35].

Penerbit
Akademia Baru

2. Mathematical Analysis

Consider the impermeable solid sphere of radius a, which is placed in an incoming stream of micropolar nanofluid with an undisturbed free-stream velocity U_∞ and constant temperature T_∞, with steady mixed convection boundary-layer flow. Two types of nanoparticles such as iron oxide (Fe₃O₄) and graphene oxide (GO) are suspended in two different types of base fluids such as methanol and kerosene oil. The convective forced flow move upward, while the gravity vector g acts downward in the opposite direction as displayed in Figure 1, where $\bar{x}$-coordinate is measured along the circumference of the solid sphere from the lower stagnation point, $\bar{y}$-coordinate is measured normal to the surface of the sphere. It is also supposed that the surface of the sphere is maintained at a constant temperature T_w with $T_w > T_\infty$ for a heated sphere (assisting flow) and $T_w < T_\infty$ for a cooled sphere (opposing flow).
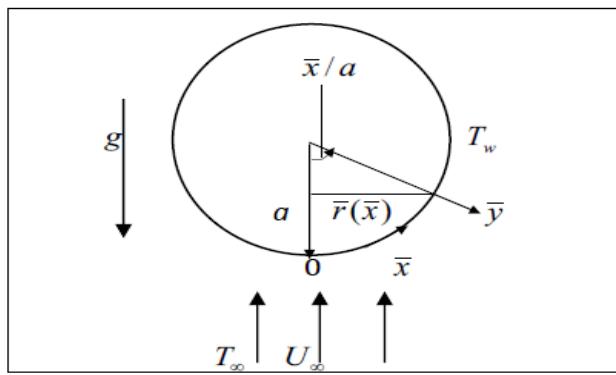

Fig. 1. Physical model and coordinate system for the mixed convection

The continuity, momentum and energy equations for micropolar nanofluid are [6]

$$\frac{\partial}{\partial \bar{x}}(\bar{r}\,\bar{u}) + \frac{\partial}{\partial \bar{y}}(\bar{r}\,\bar{v}) = 0,$$
(1)

$$\bar{u}\frac{\partial \bar{u}}{\partial \bar{x}} + \bar{v}\frac{\partial \bar{u}}{\partial \bar{y}} = \bar{u}_e\frac{d\bar{u}_e}{dx} + \left(\frac{\mu_{nf} + \kappa}{\rho_{nf}}\right)\frac{\partial^2 \bar{u}}{\partial \bar{y}^2} + \frac{\left(\chi\rho_s\beta_s + (1-\chi)\rho_f\beta_f\right)}{\rho_{nf}} g\left(T - T_\infty\right)\sin\left(\frac{\bar{x}}{a}\right) + \frac{\kappa}{\rho_{nf}}\frac{\partial \bar{H}}{\partial \bar{y}},$$
(2)

$$\rho_{nf}\, j\left(\bar{u}\frac{\partial \bar{H}}{\partial \bar{x}} + \bar{v}\frac{\partial \bar{H}}{\partial \bar{y}}\right) = -\kappa\left(2\bar{H} + \frac{\partial \bar{u}}{\partial \bar{y}}\right) + \phi_{nf}\frac{\partial^2 \bar{H}}{\partial \bar{y}^2},$$
(3)

$$\bar{u}\frac{\partial T}{\partial \bar{x}} + \bar{v}\frac{\partial T}{\partial \bar{y}} = \alpha_{nf}\frac{\partial^2 T}{\partial \bar{y}^2},$$
(4)

Subject the boundary conditions

$$\bar{u} = \bar{v} = 0,\ T = T_w,\ \bar{H} = -\frac{1}{2}\frac{\partial \bar{u}}{\partial \bar{y}}\ \text{as}\ \bar{y} = 0,$$

$$\overline{u} \to \overline{u}_e(\overline{x}), \ T \to T_\infty, \ H \to 0 \ \text{ as } \overline{y} \to \infty, \tag{5}$$

we consider that $\overline{r}(\overline{x}) = a \sin(\overline{x}/a)$ and $\overline{u}_e(\overline{x}) = \dfrac{3}{2} U_\infty \sin\left(\dfrac{\overline{x}}{a}\right)$, here $\overline{u}$ and $\overline{v}$ are the velocity

components along the $\overline{x}$ - $\overline{y}$ plane, respectively, $\overline{u}_e(\overline{x})$ is the local free-stream velocity, $\overline{r}(\overline{x})$ is the radial distance from the symmetrical axis to the surface of the sphere, T is the fluid temperature, K is the vortex viscosity, χ is the nanoparticle volume fraction, β_f is the thermal expansion coefficient of the fluid fraction, β_s is the thermal expansion coefficient of the solid fraction, α_{nf} is the thermal diffusivity of the nanofluid, ρ_{nf} is the density of the nanofluid, μ_{nf} is the viscosity of the nanofluid, $j = \dfrac{av_f}{U_\infty}$ is micro-inertia density, which are given by [36, 37]

$$\alpha_{nf} = \frac{k_{nf}}{(\rho C_p)_{nf}}, \ \rho_{nf} = (1-\chi)\rho_f + \chi\rho_f, \ \mu_{nf} = \frac{\mu_f}{(1-\chi)^{2.5}}, \ \phi_{nf} = \left(\mu_{nf} + \kappa/2\right)j,$$

$$(\rho C_p)_{nf} = (1-\chi)(\rho C_p)_f + \chi(\rho C_p)_s, \ \frac{k_{nf}}{k_f} = \frac{(k_s + 2k_f) - 2\chi(k_f - k_s)}{(k_s + 2k_f) + \chi(k_f - k_s)}, \tag{6}$$

where ϕ_{nf} is the spin gradient viscosity of nanofluid, k_{nf} is the effective thermal conductivity of the nanofluid, k_f is the thermal conductivity of the fluid, k_s is the thermal conductivity of the solid, $(\rho C_p)_{nf}$ is the heat capacity of the nanofluid, ρ_f is the density of the fluid fraction, ρ_s is the density of the solid fraction and μ_f is the viscosity of the fluid fraction.

We introduce now the following non-dimensional variables

$$x = \frac{\overline{x}}{a}, \ y = \mathrm{Re}^{1/2}\left(\frac{\overline{y}}{a}\right), \ r(x) = \frac{\overline{r}(\overline{x})}{a}, \ u = \frac{\overline{u}}{U_\infty}, \ v = \mathrm{Re}^{1/2}\left(\frac{\overline{v}}{U_\infty}\right),$$

$$H = \left(\frac{a}{U_\infty}\right)\mathrm{Re}^{1/2} \overline{H}, \ u_e(x) = \frac{\overline{u}_e(\overline{x})}{U_\infty}, \ \theta = \frac{T - T_\infty}{T_w - T_\infty}. \tag{7}$$

where $\mathrm{Re} = U_\infty \dfrac{a}{v_f}$ is the Reynolds number and v_f is the kinematic viscosity of the fluid. Substituting the previous variables into Eq. 1-4, we obtain the following boundary-layer equations for the problem under dimensionless form

$$\frac{\partial}{\partial x}\left(ru\right) + \frac{\partial}{\partial y}\left(rv\right) = 0, \tag{8}$$

$$u\frac{\partial u}{\partial x} + v\frac{\partial u}{\partial y} = u_e\frac{\partial u_e}{\partial x} + \frac{\rho_f}{\rho_{nf}}\left(D(\chi) + K\right)\frac{\partial^2 u}{\partial y^2} + \frac{1}{\rho_{nf}}\left(\chi\rho_s\left(\frac{\beta_s}{\beta_f}\right) + (1-\chi)\rho_f\right)\lambda\theta\sin x + \frac{\rho_f}{\rho_{nf}}K\frac{\partial H}{\partial y}, \tag{9}$$

$$u\frac{\partial\theta}{\partial x}+v\frac{\partial\theta}{\partial y}=\frac{1}{\Pr}\left[\frac{k_{nf}/k_f}{(1-\chi)+\chi\left(\rho c_p\right)_s/\left(\rho c_p\right)_f}\right]\frac{\partial^2\theta}{\partial y^2}, \tag{10}$$

$$u\frac{\partial H}{\partial x}+v\frac{\partial H}{\partial y}=-\frac{\rho_f}{\rho_{nf}}K\left(2\bar{H}+\frac{\partial\bar{u}}{\partial\bar{y}}\right)+\frac{\rho_f}{\rho_{nf}}\left(D(\chi)+\frac{K}{2}\right)\frac{\partial^2 H}{\partial y^2}, \tag{11}$$

where $D(\chi)=1/(1-\chi)^{2.5}$, $K=\kappa/\mu_f$ is the micro-rotation parameter, $\Pr=v_f/\alpha_f$ is the Prandtl number and λ is the mixed convection parameter, which is defined as $\lambda=Gr/\mathrm{Re}^2$ with $Gr=g\beta(T_w-T_\infty)a^3/v_f^2$ is the Grashof number. It is important mentioning that $\lambda>0$ for an assisting flow $(T_w>T_\infty)$ (heated flow), $\lambda<0$ for an opposing flow $(T_w<T_\infty)$ (cooled flow) and $\lambda=0$ the forced convection flow. The boundary conditions (5) become

$$u=v=0,\ \ \theta=1,\ \ H=-\frac{1}{2}\frac{\partial u}{\partial y}\ \ \text{as}\ \ y=0,$$

$$u\to u_e(x)=\frac{3}{2}\sin x,\ \ u\to0,\ \ \theta\to0,\ \ H\to0\ \ \text{as}\ \ y\to\infty. \tag{12}$$

We assume the following variables to solve Eq. 8-11, subject to boundary conditions (Eq. 12)

$$\psi=xr(x)f(x.y),\ \ \theta=\theta(x,y),\ \ H=xh(x,y), \tag{13}$$

where ψ is the stream function defined as

$$u=\frac{1}{r}\frac{\partial\psi}{\partial y}\ \ \text{and}\ \ v=-\frac{1}{r}\frac{\partial\psi}{\partial x},$$

which satisfies the continuity Eq. 8. Substituting the Eq. 13 into Eq. 9 to Eq. 11, we obtain the following transformed equations

$$\frac{\rho_f}{\rho_{nf}}\left(D(\chi)+K\right)\frac{\partial^3 f}{\partial y^3}+(1+x\cot x)f\frac{\partial^2 f}{\partial y^2}-\left(\frac{\partial f}{\partial y}\right)^2+\frac{1}{\rho_{nf}}\left(\chi\rho_s\left(\frac{\beta_s}{\beta_f}\right)+(1-\chi)\rho_f\right)\lambda\frac{\sin x}{x}\theta \tag{14}$$

$$+\frac{9}{4}\frac{\sin x\cos x}{x}+\frac{\rho_f}{\rho_{nf}}K\frac{\partial h}{\partial y}=x\left(\frac{\partial f}{\partial y}\frac{\partial^2 f}{\partial x\partial y}-\frac{\partial f}{\partial x}\frac{\partial^2 f}{\partial y^2}\right),$$

$$\frac{1}{\Pr}\left[\frac{k_{nf}/k_f}{(1-\chi)+\chi(\rho c_p)_s/(\rho c_p)_f}\right]\frac{\partial^2\theta}{\partial y^2}+f\frac{\partial\theta}{\partial y}(1+x\cot x)=x\left(\frac{\partial f}{\partial y}\frac{\partial\theta}{\partial x}-\frac{\partial f}{\partial x}\frac{\partial\theta}{\partial y}\right), \tag{15}$$

$$\frac{\rho_f}{\rho_{nf}}\left(D(\chi)+\frac{K}{2}\right)\frac{\partial^2 h}{\partial y^2}+(1+x\cot x)f\frac{\partial h}{\partial y}-\frac{\partial f}{\partial y}h-\frac{\rho_f}{\rho_{nf}}K\left(2h+\frac{\partial^2 f}{\partial y^2}\right)=x\left(\frac{\partial f}{\partial y}\frac{\partial h}{\partial x}-\frac{\partial f}{\partial x}\frac{\partial h}{\partial y}\right). \tag{16}$$

The boundary conditions (Eq. 12) become

$$f = \frac{\partial f}{\partial y} = 0,\ \theta = 1\ ,\ h = -\frac{1}{2}\frac{\partial^2 f}{\partial y^2}\ \text{as}\ y = 0,$$

$$\frac{\partial f}{\partial y} \to \frac{3}{2}\sin x\ \ \theta \to 0\ h \to 0\ \text{as}\ y \to \infty. \tag{17}$$

We observe that at the lower stagnation point of the sphere, $x \approx 0$ Eq. 14-17 reduce to the following differential equations

$$\frac{\rho_f}{\rho_{nf}}\left(D(\chi) + K\right)f''' + 2ff'' - \left(f'\right)^2 + \frac{1}{\rho_{nf}}\left(\chi\rho_s\left(\frac{\beta_s}{\beta_f}\right) + (1-\chi)\rho_f\right)\lambda\theta + \frac{\rho_f}{\rho_{nf}}K\frac{\partial h}{\partial y} + \frac{9}{4} = 0, \tag{18}$$

$$\frac{1}{Pr}\left[\frac{k_{nf}/k_f}{(1-\chi) + \chi\left(\rho c_p\right)_s/\left(\rho c_p\right)_f}\right]\theta'' + 2f\theta' = 0, \tag{19}$$

$$\frac{\rho_f}{\rho_{nf}}\left(D(\chi) + \frac{K}{2}\right)h'' + 2f\,h' - f'\,h - \frac{\rho_f}{\rho_{nf}}K\left(2h + f''\right) = 0, \tag{20}$$

along with the boundary conditions

$$f(0) = f'(0) = 0,\ \theta(0) = 1,\ h(0) = -\frac{1}{2}f''(0)\ \text{as}\ y = 0, \tag{21}$$

$$f' \to \frac{3}{2},\ \theta \to 0,\ h \to 0\ \text{as}\ y \to \infty,$$

where the primes denote differentiation with respect to *y*.

The physical quantities of interest are the local skin friction coefficient C_f and Nusselt number Nu and they can be written as

$$C_f = \frac{a}{\mu_f U_\infty}\text{Re}^{-1/2}\left((\mu_{nf} + \kappa)\frac{\partial\bar{u}}{\partial y} + \kappa\bar{H}\right)_{\bar{y}=0},\ \ Nu = -\frac{k_{nf}\,a}{k_f(T_w - T_\infty)}\text{Re}^{-1/2}\left(\frac{\partial T}{\partial y}\right)_{\bar{y}=0} \tag{22}$$

Using the non-dimensional variables (Eq. 7) and boundary conditions (Eq. 12) the local skin friction coefficient C_f and Nusselt number Nu are

$$C_f = \left(D(\chi) + \frac{K}{2}\right)x\frac{\partial^2 f}{\partial y^2}(x,0),\ \ Nu = -\frac{k_{nf}}{k_f}\frac{\partial\theta}{\partial y}(x,0). \tag{23}$$

3. Graphical Results and Discussion

Equations 14-16 subject to the boundary conditions (Eq. 17) have been solved numerically using an efficient implicit finite-difference scheme known as the Keller-box method, along with Newton's linearization technique as described by Cebeci *et al.,* [34]. To gain the physics of the problem, the velocity, angular velocity and temperature distribution profiles have been illustrated by varying controlling parameters, namely, mixed convection parameter λ, the micro-rotation parameter K,

and the nanoparticle volume fraction χ for both the assisting $(\lambda > 0)$ and opposing $(\lambda < 0)$ flow cases. The numerical solution starts at the lower stagnation point of the sphere, $x \approx 0$ with initial profiles as given by the Eqs. 18-21, and proceed round of the circumference of solid sphere up to the separation point. The present results are obtained up to x = 120° only. We have used data related to thermophysical properties of the fluid and nanoparticles as given in Table 1. To satisfy the accuracy of the present method, we have found the values of the heat transfer coefficient and local skin friction compared with nazar *et al.,*'s study [35] for the regular Newtonian fluid with $K = 0$ and $\chi = 0$ as presented in Table 2 and Table 3.

Table 1
Thermo-physical properties of based fluids and nanoparticles

Physical properties	Methanol	Kerosene oil	Fe_3O_4	GO
ρ (kg/m^3)	792	783	5200	1800
C_p (J/kg $-$ K)	2545	2090	670	717
k (W/m $-$ K)	0.2035	0.145	6	5000
$\beta \times 10^{-5}(K^{-1})$	149	99	1.3	28.4
Pr	7.38	21		

Table 2
Local skin friction coefficient C_f at $K = 0$ and $\chi = 0$ (Newtonian fluid), $\mathrm{Pr} = 0.7$ and various values of λ (results in parentheses are those of Nazar *et al.*, [35])

x	λ								
	-4	-3	-2	-1	-0.5	0.0	0.74	0.75	1.0
0°	(0.0000)	(0.0000)	(0.0000)	(0.0000)	(0.0000)	(0.0000)	(0.0000)	(0.0000)	(0.0000)
	(0.0000)	(0.0000)	(0.0000)	(0.0000)	(0.0000)	(0.0000)	(0.0000)	(0.0000)	(0.0000)
10°	0.07987	0.1806	0.2665	0.3443	0.3810	0.4166	0.46761	0.4682	0.4850
	(0.0801)	(0.1806)	(0.2662)	(0.3438)	(0.3804)	(0.4160)	(0.4669)	(0.4675)	(0.4843)
20°	0.1152	0.3269	0.5016	0.6583	0.7320	0.8034	0.9053	0.9067	0.9400
	(0.1149)	(0.3261)	(0.5000)	(0.6564)	(0.7301)	(0.8014)	(0.9031)	(0.9045)	(0.9380)
30°		0.4043	0.6754	0.9138	1.0253	1.2110	1.2858	1.2878	1.3375
		(0.4024)	(0.6718)	(0.9098)	(1.0211)	(1.1284)	(1.2813)	(1.2833)	(1.3335)
40°		0.3737	0.7602	1.0860	1.2363	1.3806	1.5851	1.5878	1.6534
		(0.3704)	(0.7535)	(1.0790)	(1.2292)	(1.3733)	(1.5775)	(1.5802)	(1.6471)
50°			0.7199	1.1540	1.3457	1.5281	1.7848	1.7882	1.8690
			(0.7181)	(1.1434)	(1.3350)	(1.5172)	(1.7737)	(1.7771)	(1.8607)
60°			0.5466	1.1014	1.3392	1.5623	1.8729	1.8770	1.9659
			(0.5295)	(1.0866)	(1.3246)	(1.4577)	(1.8580)	(1.8621)	(1.9627)
70°				0.9127	1.2078	1.4727	1.8550	1.8493	1.9703
				(0.8929)	(1.1889)	(1.4583)	(1.8260)	(1.8307)	(1.9486)
80°				0.5545	0.9326	1.2705	1.7023	1.7078	1.8307
				(0.5280)	(0.9190)	(1.2480)	(1.6800)	(1.6855)	(1.8216)
90°					0.5243	0.9305	1.4573	1.4638	1.6061
					(0.4813)	(0.9154)	(1.4289)	(1.4352)	(1.5915)
100°						0.4612	1.1245	1.1321	1.2874
						(0.4308)	(1.0847)	(1.0922)	(1.2732)
110°							0.7003	0.7001	0.8960
							(0.6543)	(0.6637)	(0.8831)
120°								0.0427	0.4327
								(0.0380)	(0.4220)

Table 3

Local Nusselt number Nu at $K=0$ and $\chi=0$ (Newtonian fluid), $\Pr=0.7$ and various values of λ (results in parentheses are those of Nazar *et al.*, [35])

x	λ								
	-4	-3	-2	-1	-0.5	0.0	0.74	0.75	1.0
0°	0.6518	0.7094	0.7516	0.7858	0.8009	0.8149	0.8342	0.8344	0.8406
	(0.6534)	(0.7108)	(0.7529)	(0.7870)	(0.8021)	(0.8162)	(0.8354)	(0.8357)	(0.8463)
10°	0.6430	0.7030	0.7462	0.7809	0.7961	0.8103	0.8298	0.8300	0.8362
	(0.6440)	(0.7040)	(0.7470)	(0.7818)	(0.7970)	(0.8112)	(0.8307)	(0.8309)	(0.8371)
20°	0.6146	0.6839	0.7301	0.7664	0.7822	0.7969	0.8168	0.8171	0.8233
	(0.6150)	(0.6845)	(0.7305)	(0.7669)	(0.7827)	(0.7974)	(0.8173)	(0.8176)	(0.8239)
30°		0.6504	0.7031	0.7424	0.7592	0.7747	0.7955	0.7958	0.8021
		(0.6507)	(0.7027)	(0.7422)	(0.7591)	(0.7746)	(0.7955)	(0.7958)	(0.8024)
40°		0.5981	0.6640	0.7086	0.7270	0.7437	0.7659	0.7662	0.7677
		(0.5977)	(0.6628)	(0.7076)	(0.7261)	(0.7429)	(0.7652)	(0.7655)	(0.7725)
50°			0.6106	0.6643	0.6853	0.7038	0.7281	0.7284	0.7351
			(0.6080)	(0.6624)	(0.6836)	(0.7022)	(0.7267)	(0.7270)	(0.7345)
60°			0.5382	0.6085	0.6335	0.6550	0.6822	0.6825	0.6896
			(0.5309)	(0.6055)	(0.6309)	(0.6525)	(0.6800)	(0.6803)	(0.6887)
70°				0.5379	0.57071	0.5968	0.6284	0.6287	0.6365
				(0.5224)	(0.5668)	(0.5934)	(0.6253)	(0.6257)	(0.6352)
80°				0.4395	0.4915	0.5264	0.5650	0.5655	0.5759
				(0.4342)	(0.4879)	(0.5236)	(0.5672)	(0.5632)	(0.5742)
90°					0.3817	0.4353	0.4862	0.4868	0.5080
					(0.3796)	(0.4398)	(0.4920)	(0.4926)	(0.5060)
100°						0.3196	0.3924	0.4000	0.4326
						(0.3263)	(0.4120)	(0.4127)	(0.4304)
110°							0.3132	0.2985	0.3481
							(0.3179)	(0.3192)	(0.3458)
120°								0.1936	0.24682
								(0.1276)	(0.2442)

The effect of nanoparticle volume fraction χ, the micro-rotation parameter K, and the mixed convection parameter λ on local skin friction C_f and local Nusselt number Nu for Fe_3O_4 and GO suspended methanol-kerosene oil base nanofluids shown in Figures 2 to 7, respectively. We notice that the local Nusselt number Nu and the local skin friction coefficient C_f increase with increasing values of nanoparticle volume fraction x, the micro-rotation parameter K and the mixed convection parameter λ. It is also noticed that Fe_3O_4/GO kerosene oil has higher in local Nusselt number compared with Fe_3O_4/GO methanol for various values of nanoparticle volume fraction x, the micro-rotation parameter K and the mixed convection parameter λ. Further, the local skin friction C_f of Fe_3O_4/GO methanol is higher than Fe_3O_4/GO kerosene oil for nanoparticle volume fraction χ, the micro-rotation parameter K and the mixed convection parameter $(\lambda>0)$. On the other hand, the opposite effect happened when $(\lambda<0)$, the local skin friction of Fe_3O_4/GO methanol is lower than Fe_3O_4/GO kerosene oil, this is because of the physical properties for fluids. Moreover, these figures showed that the local Nusselt number Nu and the local skin friction C_f of graphene oxide is higher than the iron oxide with increase values of nanoparticle volume fraction x, the micro-rotation parameter K and the mixed convection parameter $(\lambda>0)$ and in the opposite case, the graphene oxide has low local Nusselt number Nu and local skin friction C_f as compare to iron oxide when the

mixed convection parameter $(\lambda < 0)$. Also, it is observed from these figures for Fe_3O_4/GO nanoparticles suspends in two based fluids namely methanol and kerosene oil, that the actual value of $\lambda = \lambda_s (> 0)$, which first gives no separation, is difficult to determine precisely as it has to be found by successive integrations of the equations. However, the numerical solutions indicate that the value of λ_s, which first gives no separation, lies between 0.75 and 1.0 for $\chi = 0.1$ and $K = 0.2$.
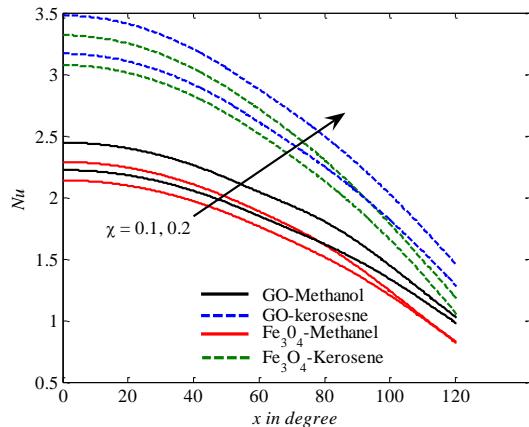
Fig. 2. Variation of the local Nusselt number using Fe_3O_4/GO methanol and kerosene oil-based nanofluids, for various values of *x* and χ when $\lambda = 3$ and $K = 0.2$
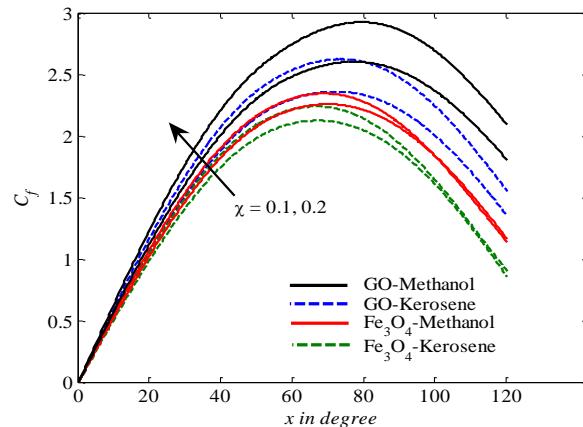
Fig. 3. Variation of the local skin friction using Fe_3O_4/GO methanol and kerosene oil-based nanofluids, for various values of *x* and χ, when $\lambda = 3$ and $K = 0.2$
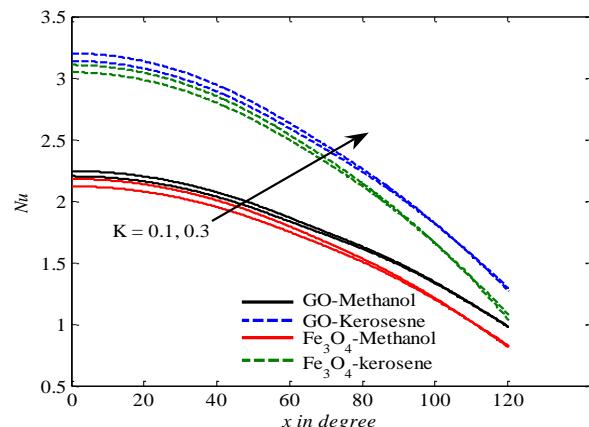

Fig. 4. Variation of the local Nusselt number using Fe_3O_4/GO in methanol and kerosene oil-based nanofluids, for various values of *x* and K, when $\lambda = 3$ and $\chi = 0.1$
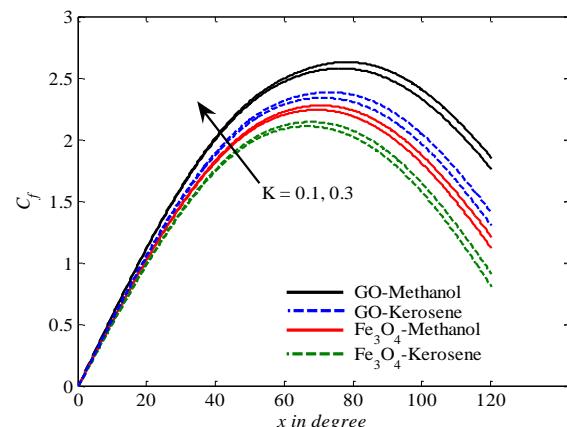
**Fig. 5.** Variation of the local skin friction using Fe_3O_4/GO methanol and kerosene oil-based nanofluids, for various values of *x* and K, when $\lambda = 3$ and $\chi = 0.1$

Figures 8 to 16 show the temperature, velocity and angular velocity profiles respectively, at the lower stagnation point of the sphere, $x \approx 0$, for nanoparticle volume fraction χ, the micro-rotation parameter K, and the mixed convection parameter λ for both Fe_3O_4 and GO suspended nanoparticles in methanol and kerosene oil. It can be seen that when the χ and the K increase, the

velocity profiles and the angular velocity profiles decrease, but the temperature profiles increase. It is also found that the temperature is decrease, and the velocity and the angular increase when the mixed convection parameter λ increase. Besides that, it is also noticed that Fe_3O_4/GO methanol has a higher temperature, velocity and angular velocity compared with Fe_3O_4/GO kerosene oil for every values of nanoparticle volume fraction χ, the micro-rotation parameter K and the mixed convection parameter $(\lambda > 0)$. On the other hand, the opposite case happens when $(\lambda < 0)$, the velocity and the angular velocity of Fe_3O_4/GO methanol is lower than Fe_3O_4/GO kerosene oil.
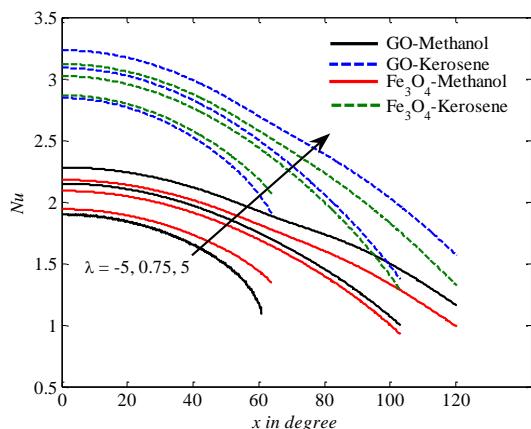
Fig. 6. Variation of the local Nusselt number using Fe_3O_4/GO methanol and kerosene oil-based nanofluids, for various values of *x* and λ, when $K = 0.2$ and $\chi = 0.1$
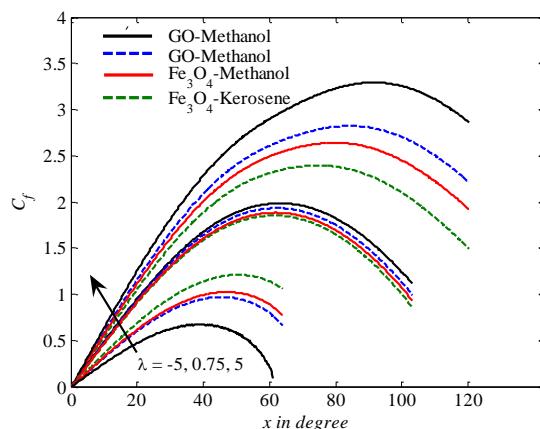
Fig. 7. Variation of the local skin friction using Fe_3O_4/GO methanol and kerosene oil-based nanofluids, for various values of *x* and λ, when $K = 0.2$ and $\chi = 0.1$
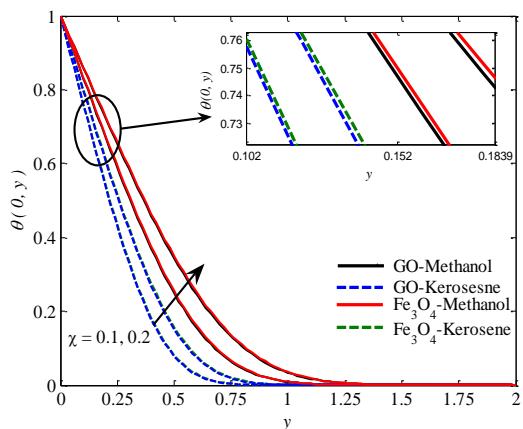
Fig. 8. Temperature profiles at $x \approx 0$ using Fe_3O_4/GO methanol and kerosene oil-based nanofluids, for various values of χ, when $\lambda = 3$ and $K = 0.2$
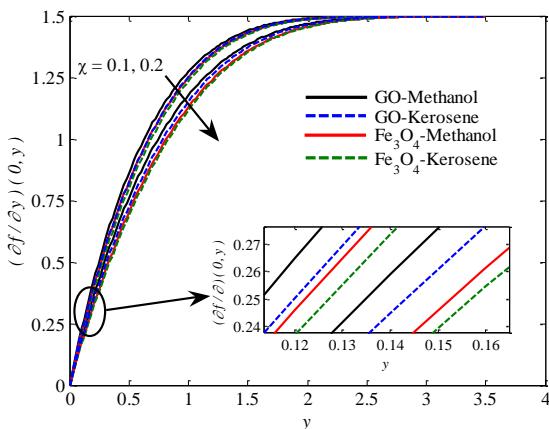
**Fig. 9.** Velocity profiles at $x \approx 0$ using Fe_3O_4/GO methanol and kerosene oil-based nanofluids, for various values of χ, when $\lambda = 3$ and $K = 0.2$
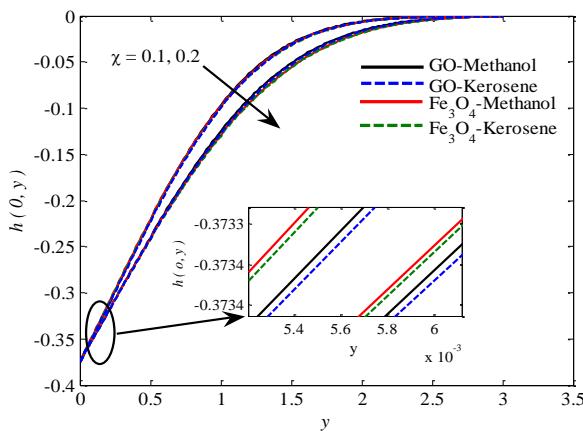
Fig. 10. Angular velocity profiles at $x \approx 0$ using Fe_3O_4/GO methanol and kerosene oil-based nanofluids, for various values of χ, when $\lambda = 3$ and $K = 0.2$
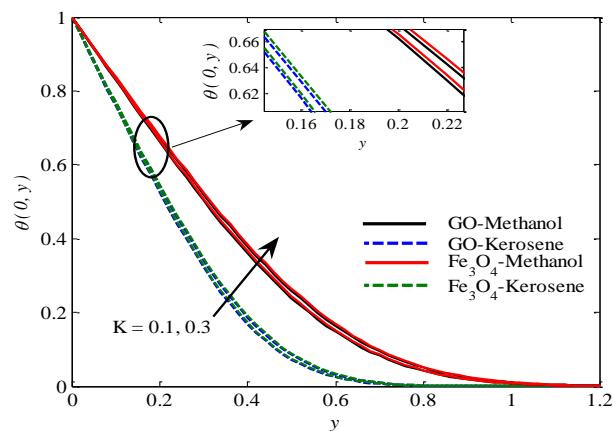
Fig. 11. Temperature profiles at $x \approx 0$ using Fe_3O_4/GO methanol and kerosene oil-based nanofluids, for various values of K, when $\lambda = 3$ and $\chi = 0.1$
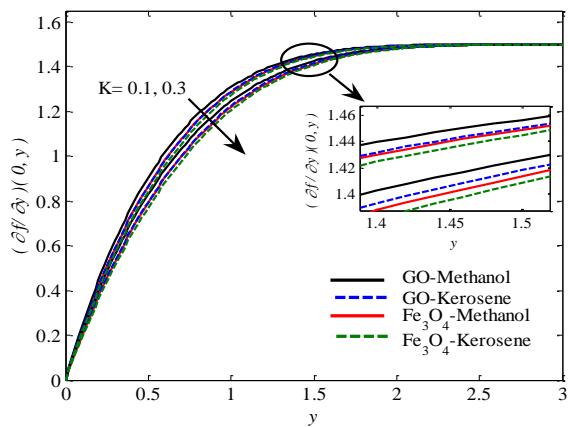
**Fig. 12.** Velocity profiles at $x \approx 0$ using Fe_3O_4/GO methanol and kerosene oil-based nanofluids, for various values of K, when $\lambda = 3$ and $\chi = 0.1$
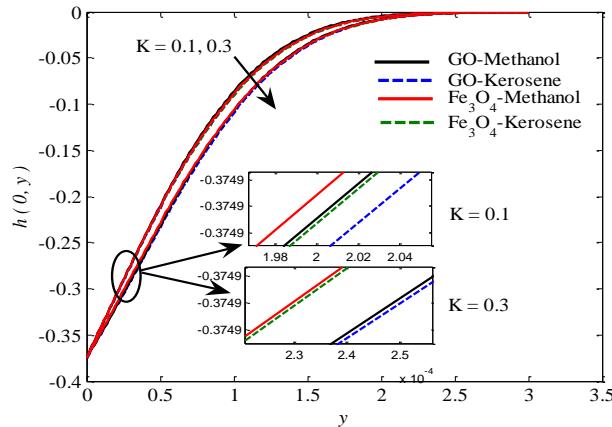
Fig. 13. Angular velocity profiles at $x \approx 0$ using Fe_3O_4/GO methanol and kerosene oil-based nanofluids, for various values of K, when $\lambda = 3$ and $\chi = 0.1$
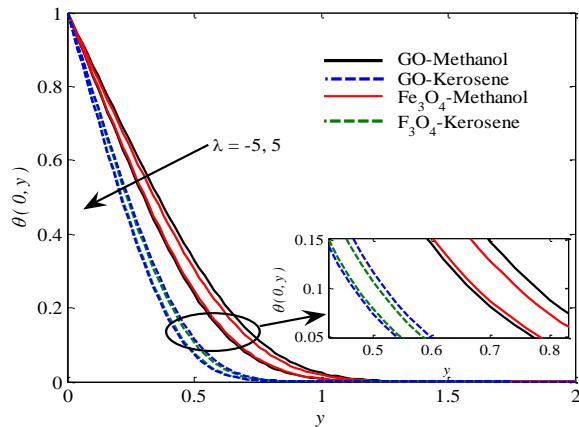

Fig. 14. Temperature profiles at $x \approx 0$ using Fe_3O_4/GO methanol and kerosene oil-based nanofluids, for various values of λ, when $K = 0.2$ and $\chi = 0.1$
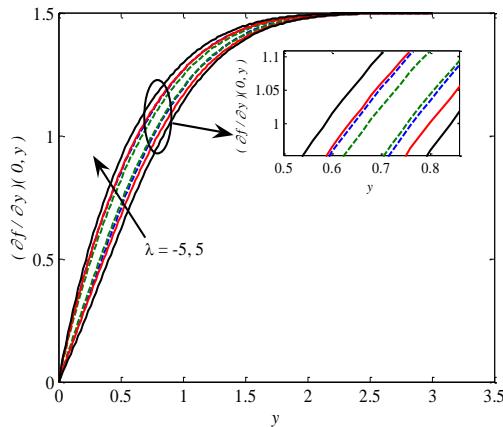

Fig. 15. Velocity profiles at $x \approx 0$ using Fe_3O_4/GO methanol and kerosene oil-based nanofluids, for various values of λ, when $K = 0.2$ and $\chi = 0.1$
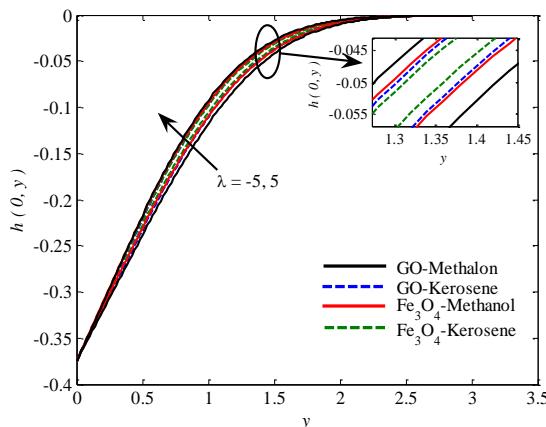
Fig. 16. Angular velocity profiles at $x \approx 0$ using $\mathrm{Fe_3O_4/GO}$ methanol and kerosene oil-based nanofluids, for various values of λ, when $K = 0.2$ and $\chi = 0.1$

4. Conclusions

In this paper, we have numerically studied the mixed convection boundary-layer flow about an isothermal solid sphere in a micropolar nanofluid with constant wall temperature. We discussed the effects of the mixed convection parameter λ, the nanoparticle volume fraction χ, the micro-rotation parameter K and the type of nanoparticles Fe₃O₄ and GO suspended in two based fluids such as methanol and kerosene oil. From this study, the following results obtained

i. An increase in the value of the nanoparticle volume fraction χ, the micro-rotation parameter K and the mixed convection parameter λ, led to an increase of both the local Nusselt number Nu and the local skin friction coefficient C_f

ii. The $\mathrm{Fe_3O_4/GO}$ kerosene oil has higher in local Nusselt number compared with $\mathrm{Fe_3O_4/GO}$ methanol for various values of χ, K and λ.

iii. An increase in the value of the parameters χ and K led to a decrease in the velocity profiles and the angular velocity profiles, but the temperature profiles increase.

iv. $\mathrm{Fe_3O_4/GO}$ methanol has a higher temperature, velocity and angular velocity compared with $\mathrm{Fe_3O_4/GO}$ kerosene oil for every value of parameters χ and K.

References
[1]   Das, Sarit K., Stephen U. Choi, Wenhua Yu, and T. Pradeep. *Nanofluids: science and technology.* John Wiley & Sons, 2007.
[2]   Abu-Nada, Eiyad, and Hakan F. Oztop. "Effects of inclination angle on natural convection in enclosures filled with Cu–water nanofluid." *International Journal of Heat and Fluid Flow* 30, no. 4 (2009): 669-678.
[3]   Wang, Xiang-Qi, and Arun S. Mujumdar. "Heat transfer characteristics of nanofluids: a review." *International journal of thermal sciences* 46, no. 1 (2007): 1-19.

[4] Kakaç, Sadik, and Anchasa Pramuanjaroenkij. "Review of convective heat transfer enhancement with nanofluids." *International Journal of Heat and Mass Transfer* 52, no. 13-14 (2009): 3187-3196.

[5] Buongiorno, Jacopo. "Convective transport in nanofluids." *Journal of heat transfer* 128, no. 3 (2006): 240-250.

[6] Tiwari, Raj Kamal, and Manab Kumar Das. "Heat transfer augmentation in a two-sided lid-driven differentially heated square cavity utilizing nanofluids." *International Journal of Heat and Mass Transfer* 50, no. 9-10 (2007): 2002-2018.

[7] Godson, Lazarus, B. Raja, D. Mohan Lal, and S. Wongwises. "Enhancement of heat transfer using nanofluids—an overview." *Renewable and sustainable energy reviews* 14, no. 2 (2010): 629-641.

[8] Kandelousi, Mohsen Sheikholeslami. "KKL correlation for simulation of nanofluid flow and heat transfer in a permeable channel." *Physics Letters A* 378, no. 45 (2014): 3331-3339.

[9] Haq, Rizwan Ul, Sohail Nadeem, Zafar Hayyat Khan, and N. F. M. Noor. "Convective heat transfer in MHD slip flow over a stretching surface in the presence of carbon nanotubes." *Physica B: condensed matter* 457 (2015): 40-47.

[10] Abu-Nada, Eiyad. "Application of nanofluids for heat transfer enhancement of separated flows encountered in a backward facing step." *International Journal of Heat and Fluid Flow* 29, no. 1 (2008): 242-249.

[11] Oztop, Hakan F., and Eiyad Abu-Nada. "Numerical study of natural convection in partially heated rectangular enclosures filled with nanofluids." *International journal of heat and fluid flow* 29, no. 5 (2008): 1326-1336.

[12] A. Hussanan, S. Aman, Z. Ismail, M. Z.Salleh, B. Widodo, "Unsteady natural convection of sodium alginate viscoplastic Casson based nanofluid flow over a vertical plate with leading edge accretion/ablation," *Journal of Advanced Research in Fluid Mechanics and Thermal Sciences*, vol. 45 (2018): 92-98.

[13] Kandelousi, Mohsen Sheikholeslami. "Effect of spatially variable magnetic field on ferrofluid flow and heat transfer considering constant heat flux boundary condition." *The European Physical Journal Plus* 129, no. 11 (2014): 248.

[14] Qasim, M., Z. H. Khan, R. J. Lopez, and W. A. Khan. "Heat and mass transfer in nanofluid thin film over an unsteady stretching sheet using Buongiorno's model." *The European Physical Journal Plus* 131, no. 1 (2016): 16.

[15] Hussanan, Abid, Ilyas Khan, Hasmawani Hashim, Muhammad Khairul Anuar Mohamed, Nazila Ishak, Norhafizah Md Sarif, and Mohd Zuki Salleh. "Unsteady MHD flow of some nanofluids past an accelerated vertical plate embedded in a porous medium." *Journal Teknologi* 78, no. 2 (2016).

[16] Hussanan, Abid, Mohd Zuki Salleh, Ilyas Khan, and Sharidan Shafie. "Convection heat transfer in micropolar nanofluids with oxide nanoparticles in water, kerosene and engine oil." *Journal of Molecular Liquids* 229 (2017): 482-488.

[17] Eringen, A. Cemal. "Theory of micropolar fluids." *Journal of Mathematics and Mechanics* (1966): 1-18.

[18] Hassanien, I. A., A. A. Abdullah, and R. S. R. Gorla. "Numerical solutions for heat transfer in a micropolar fluid over a stretching sheet." *Applied Mechanics and Engineering* 3, no. 3 (1998): 377-391.

[19] Papautsky, Ian, John Brazzle, Timothy Ameel, and A. Bruno Frazier. "Laminar fluid behavior in microchannels using micropolar fluid theory." *Sensors and actuators A: Physical* 73, no. 1-2 (1999): 101-108.

[20] Nazar, Roslinda, Norsarahaida Amin, Diana Filip, and Ioan Pop. "Stagnation point flow of a micropolar fluid towards a stretching sheet." *International Journal of Non-Linear Mechanics* 39, no. 7 (2004): 1227-1235.

[21] Sherief, H. H., M. S. Faltas, and E. A. Ashmawy. "Exact solution for the unsteady flow of a semi-infinite micropolar fluid." *Acta Mechanica Sinica* 27, no. 3 (2011): 354-359.

[22] Hussanan, Abid, Mohd Zuki Salleh, Ilyas Khan, and Razman Mat Tahar. "Heat and mass transfer in a micropolar fluid with Newtonian heating: an exact analysis." *Neural Computing and Applications* 29, no. 6 (2018): 59-67.

[23] Hussanan, Abid, Mohd Zuki Salleh, Ilyas Khan, and Razman Mat Tahar. "UNSTEADY FREE CONVECTION FLOW OF A MICROPOLAR FLUID WITH NEWTONIAN HEATING: Closed Form Solution." *Thermal Science* 21, no. 6 (2017).

[24] Alkasasbeh, Hamzeh Taha, Mohd Zuki Salleh, Razman Mat Tahar, Roslinda Nazar, and Ioan Pop. "Free Convection Boundary Layer Flow on a Solid Sphere with Convective Boundary Conditions in a Micropolar Fluid." *World Applied Sciences Journal* 32, no. 9 (2014): 1942-1951.

[25] Alkasasbeh, Hamzeh. "NUMERICAL SOLUTION ON HEAT TRANSFER MAGNETOHYDRODYNAMIC FLOW OF MICROPOLAR CASSON FLUID OVER A HORIZONTAL CIRCULAR CYLINDER WITH THERMAL RADIATION." *Frontiers in Heat and Mass Transfer (FHMT)* 10 (2018).

[26] Swalmeh, Mohammed Z., Hamzeh T. Alkasasbeh, Abid Hussanan, and Mustafa Mamat. "Heat transfer flow of Cu-water and Al2O3-water micropolar nanofluids about a solid sphere in the presence of natural convection using Keller-box method." *Results in Physics* 9 (2018): 717-724.

[27] Waqas, Hassan, Sajjad Hussain, Humaira Sharif, and Shamila Khalid. "MHD forced convective flow of micropolar fluids past a moving boundary surface with prescribed heat flux and radiation." *Br. J. Math. Comput. Sci.* 21 (2017): 1-14.

[28] Yuge, T. "Experiments on heat transfer from spheres including combined natural and forced convection." *Journal of Heat Transfer* 82, no. 3 (1960): 214-220.

[29] Hieber, C. A., and B. Gebhart. "Mixed convection from a sphere at small Reynolds and Grashof numbers." *Journal of Fluid Mechanics* 38, no. 1 (1969): 137-159.

[30] Chen, T. S., and Aleksandros Mucoglu. "Analysis of mixed forced and free convection about a sphere." *International Journal of Heat and Mass Transfer* 20, no. 8 (1977): 867-875.

[31] Dennis, S. C. R., and J. D. A. Walker. "Calculation of the steady flow past a sphere at low and moderate Reynolds numbers." *Journal of Fluid Mechanics* 48, no. 4 (1971): 771-789.

[32] Tham, L., R. Nazar, and I. Pop. "Mixed convection boundary-layer flow about an isothermal solid sphere in a nanofluid." *Physica Scripta* 84, no. 2 (2011): 025403.

[33] Alkasasbeh, Hamzeh Taha, M. Z. Salleh, R. M. Tahar, R. Nazar, and I. Pop. "Numerical Solution for Mixed Convection Boundary Layer Flow About a Solid Sphere in a Micropolar Fluid with Convective Boundary Conditions." *World Applied Sciences Journal* 33, no. 9 (2015): 1472-1481.

[34] Cebeci, Tuncer, and Peter Bradshaw. *Physical and computational aspects of convective heat transfer.* Springer Science & Business Media, 2012.

[35] Nazar, Roslinda, Norsarahaida Amin, and Ioan Pop. "Mixed convection boundary layer flow about an isothermal sphere in a micropolar fluid." *International journal of thermal sciences* 42, no. 3 (2003): 283-293.

[36] Hussanan, Abid, Mohd Zuki Salleh, and Ilyas Khan. "Microstructure and inertial characteristics of a magnetite ferrofluid over a stretching/shrinking sheet using effective thermal conductivity model." *Journal of Molecular Liquids* 255 (2018): 64-75.

[37] H. T. Alkasasbeh, " Numerical solution of micropolar Casson fluid behaviour on steady MHD natural convective flow about a solid sphere," *Journal of Advanced Research in Fluid Mechanics and Thermal Sciences* 50, no. 1 (2018): 55-66.